BIOCELL
2022 46(11): 2507-2515

Tech Science Press

In vivo protective effect of late embryogenesis abundant protein ($ApSK_3$ dehydrin) on *Agapanthus praecox* to promote post-cryopreservation survival

TINGTING HUANG[1,#]; SHAN DENG[2,#]; JIANGYUAN SHENG[1]; DI ZHANG[1,*]

[1] Department of Landscape Science and Engineering, School of Design, Shanghai Jiao Tong University, Shanghai, 200240, China
[2] Institute for Agri-Food Standards and Testing Technology, Shanghai Academy of Agricultural Sciences, Shanghai, 201403, China

Key words: Dehydrin, Embryogenic callus, Cryopreservation, RNAi, Gene overexpression

Abstract: Dehydrins (DHNs), as members of the late embryogenesis abundant protein family, play critical roles in the protection of seeds from dehydration and plant adaptation to multiple abiotic stresses. Vitrification is a basic method in plant cryopreservation and is characterized by forming a glassy state to prevent lethal ice crystals produced during cryogenic storage. In this study, $ApSK_3$ type DHN was genetically transformed into embryogenic calluses (EC) of *Agapanthus praecox* by overexpression (OE) and RNA interference (RNAi) techniques to evaluate the *in vivo* protective effect of DHNs during cryopreservation. The cell viability showed a completely opposite trend in OE and RNAi cell lines, the cell relative death ratio was decreased by 20.0% in $ApSK_3$-OE EC and significantly increased by 66.15% in $ApSK_3$-RNAi cells after cryopreservation. Overexpression of $ApSK_3$ increased the content of non-enzymatic antioxidants (AsA and GSH) and up-regulated the expression of *CAT, SOD, POD,* and *GPX* genes, while $ApSK_3$-RNAi cells decreased antioxidant enzyme activities and *FeSOD, POD,* and *APX* genes expression during cryopreservation. These findings suggest that $ApSK_3$ affects ROS metabolism through chelating metal ions (Cu^{2+} and Fe^{3+}), alleviates H_2O_2 and OH· excessive generation, activates the antioxidant system, and improves cellular REDOX balance and membrane lipid peroxidation damage of plant cells during cryopreservation. DHNs can effectively improve cell stress tolerance and have great potential for *in vivo* or *in vitro* applications in plant cryopreservation.

Introduction

Cryopreservation provides a safe and cost-effective *in vitro* method for the long-term preservation of plant genetic resources (Ren *et al.*, 2021). Vitrification, dehydration-encapsulation, and controlled freezing are commonly used methods for plant cryopreservation (Reed, 2001). Vitrification is widely used in plant cryopreservation because of its rapid and convenient operation (Ren *et al.*, 2013). The basic principle of the vitrification procedure is to prevent the formation of lethal ice crystals within the cell (Sakai *et al.*, 2008; Zamecnik *et al.*, 2021). Cryoprotectant treatment can lead to continuous dehydration of plant cells, increase cytoplasmic viscosity and achieve a glassy state, which is important for cell survival during vitrification cryopreservation (Meryman, 2007). However, cryopreservation treatments can also cause severe complex stresses to preserved cells, including dehydration and osmotic damage, oxidative stress, lipid membrane damage, protein aggregation, and ion toxicity (Meryman, 2007; Ren *et al.*, 2013; Ren *et al.*, 2021; Fayter *et al.*, 2020; Elliott *et al.*, 2017).

Antioxidant systems, including superoxide dismutase (SOD), peroxidase (POD), the ascorbic acid (AsA)-glutathione (GSH) cycle, and the glutathione peroxidase (GPX) cycle, are involved in removing excessive reactive oxygen species (ROS) and alleviating oxidative stress damage during cryopreservation procedure (Ren *et al.*, 2015; Zhang *et al.*, 2015). Ren *et al.* (2014) used some exogenous regulatory substances to alleviate the cell oxidative stress and optimize the cryopreservation system and found that GSH, AsA, abscisic acid, and glycine betaine can effectively increase the rate of survival post-cryopreservation. Nowadays, the promotion of the post-cryopreservation survival or regeneration of plants after cryopreservation is still a significant scientific issue in cryobiology.

Living cells are not tolerant of dehydration. Orthodox seeds (desiccation-tolerant seeds), as a special case, lose most water achieving the glassy state and can be stored for a

*Address correspondence to: Di Zhang, zhangdi2013@sjtu.edu.cn
#Authors contributed equally to this work
Received: 08 January 2022; Accepted: 11 April 2022

Doi: 10.32604/biocell.2022.021314

long term (Hoekstra *et al.*, 2001; Smolikova *et al.*, 2020). Late embryogenesis abundant (LEA) proteins are highly abundant during the later stages of seed maturation to endow the seeds with drought tolerance ability (Liu *et al.*, 2013; Avelange-Macherel *et al.*, 2015; Bao *et al.*, 2017). In the last decade, some studies found that in addition to protecting the seeds from dehydration, LEA protein is also induced by water-related abiotic stress in a wide range of vegetative tissues and organisms (Saibi *et al.*, 2015; Saucedo *et al.*, 2017). Dehydrins (DHNs), the group II LEA proteins, are one of the most functional members of the LEA family (Close, 1997). DHNs are disordered proteins and have highly hydrophilic and flexible structures (Hara *et al.*, 2016; Hughes *et al.*, 2013). This special structure enables DHNs to maintain stability even at high temperatures, such as in boiling water or at freezing temperatures (Livernois *et al.*, 2009; Saucedo *et al.*, 2017; Yang *et al.*, 2019). DHNs protect biomacromolecules by nonspecific binding mode, called 'molecular shield' (Hughes *et al.*, 2013). Several studies have reported that under different environmental stresses, DNH is able to directly bind to the metal ions to reduce the ROS, prevent membrane and protein aggregation (Halder *et al.*, 2016, 2017; Rakhra *et al.*, 2017), and protect the integrity of biomolecules (Abdul *et al.*, 2021). In our previous studies, two DHNs ($ApSK_3$ and ApY_2SK_2) as protective proteins were screened in embryogenic callus (EC) of *Agapanthus praecox* during cryopreservation by combined RNA-seq and proteomics analysis. *In vitro* protein functional analysis indicated that ApY_2SK_2 and $ApSK_3$ can effectively protect enzyme activity and significantly inhibit hydroxyl radical (OH·) generation during the freeze-thaw process (Yang *et al.*, 2019). Furthermore, we purified ApY_2SK_2 and $ApSK_3$ proteins by prokaryotic expression method and added them to PVS2. The results showed that the survival rate of *Arabidopsis thaliana* seedlings increased approximately by 100% after adding DHNs compared to the control group after cryopreservation (Zhang *et al.*, 2021). However, *in vivo* protective effects of DHNs on cryopreservation have not yet been fully elucidated.

In this study, ECs of *Agapanthus praecox* were genetically transformed for $ApSK_3$ overexpression or silencing through RNA interference (RNAi). Cryopreservation and stress physiological tests were performed on transgenic EC to evaluate the *in vivo* protective effect of DHNs during cryopreservation and obtain a novel insight for the *in vivo* or *in vitro* application of DHNs to optimize cryopreservation techniques.

Results

The pHB-YFP-$ApSK_3$ (Overexpression) and pTCK303-$ApSK_3$-GUS (RNAi) were transferred into *Agrobacterium tumefaciens* (GV3101), which was then co-cultured and allowed to infect EC of *Agapanthus praecox* for 5 d (Figs. 1a and 1e). The transgenic cells were screened using carboxypenicillin and hygromycin. Most ECs showed browning and gradually died after 4–8 weeks of hygromycin screening (Figs. 1b, 1c, 1f and 1g). The transgenic EC proliferated gradually and were clearly differentiated from the browning cells after 12 weeks of hygromycin screening (Figs. 1d and 1h).

Yellow fluorescence protein (YFP) signals and histochemical β-glucuronidase (GUS) staining results showed that $ApSK_3$ was successfully transformed and stably expressed in EC cells (Figs. 2a and 2b). The gene expression level of $ApSK_3$-OE and $ApSK_3$-RNAi cell lines were 126%–162% and 71%–84% of that of control EC, respectively (Fig. 2c). The western blot test showed stable expression of $ApSK_3$ protein in each transgenic cell line (Fig. 2d). These results suggested that $ApSK_3$-OE and $ApSK_3$-RNAi transgenic EC could be used for subsequent experiments on the evaluation of cryopreservation and stress physiology.

$ApSK_3$ can significantly improve the cell viability and antioxidant system, and alleviate oxidative stress damage during

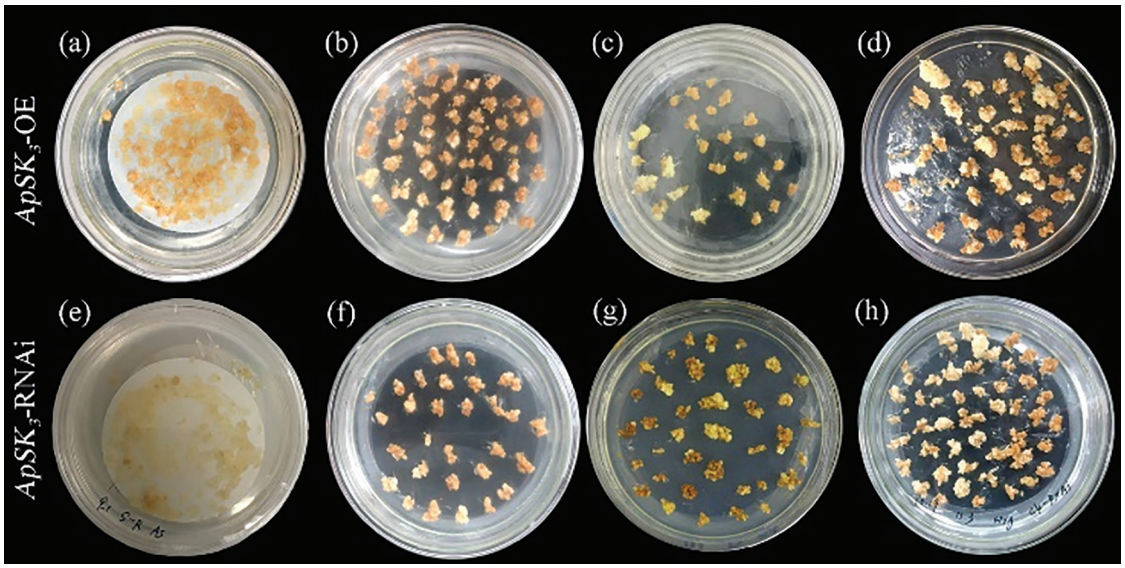

FIGURE 1. Transgenic embryogenic callus of *Agapanthus praecox* screening with hygromycin. (a–d) Overexpression of late embryogenesis abundant protein $ApSK_3$ ($ApSK_3$-OE); (e–f) RNA interference of $ApSK_3$; (a, e) Embryogenic callus (EC) and *Agrobacterium tumefaciens* co-culture stage; (b, f) Hygromycin resistance was screened for 4 weeks; (c, g) Hygromycin resistance was screened for 8 weeks; (d, h) Hygromycin resistance was screened for 12 weeks.

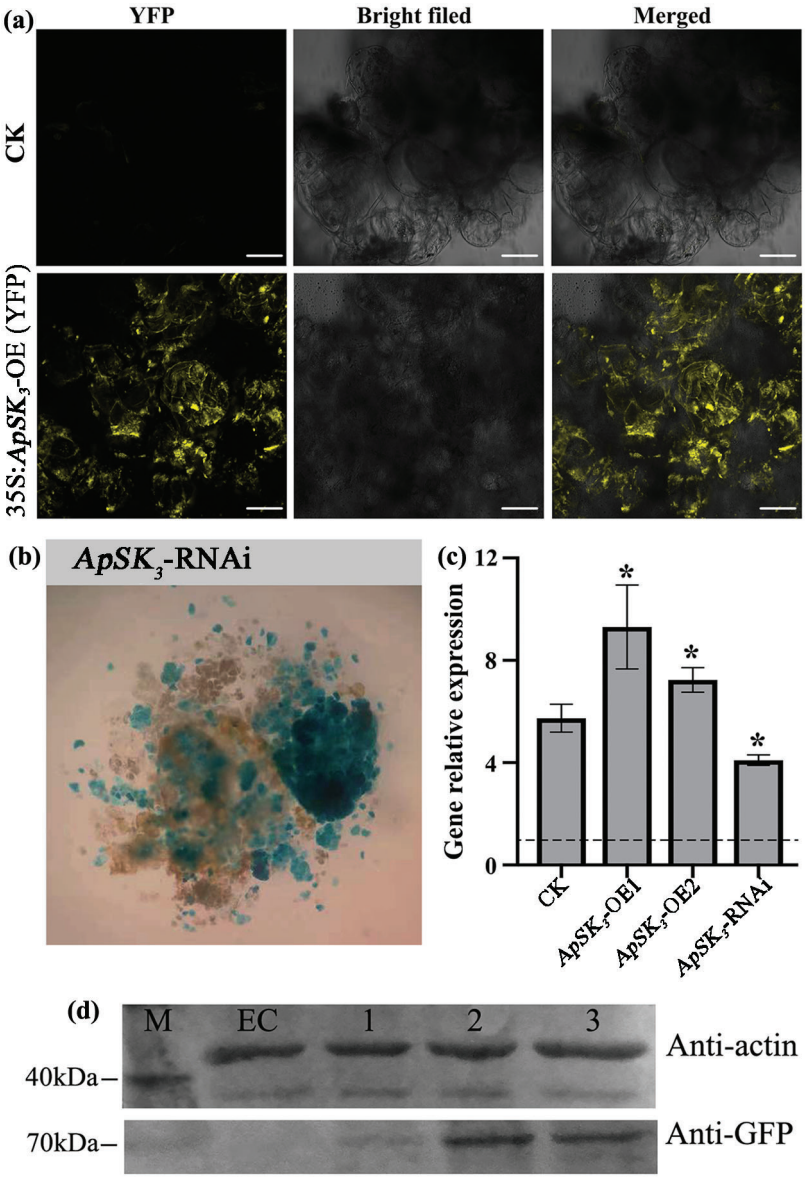

FIGURE 2. Detection of *ApSK$_3$* overexpression and RNAi transgenic *Agapanthus praecox* embryogenic callus. (a) Confocal microscopy images of overexpressed ApSK$_3$-YFP fusion protein in embryogenic callus (EC). Bar = 50 μm; (b) GUS staining of ApSK$_3$ RNAi transgenic EC; (c) Real-time quantitative polymerase chain reaction detection of *ApSK$_3$* overexpression and RNAi transgenic *Agapanthus praecox* EC, the dotted line represents the expression level of the housekeeping gene Actin; (d) Western blot results of ApSK$_3$ overexpression transgenic *Agapanthus praecox* EC (lanes 1–3: overexpressing cell lines). *$P < 0.05$.

cryopreservation. The results of 2,3,5-triphenyltetrazolium chloride (TTC) staining showed that the cell viability of the three genotypes had no significant difference before cryopreservation. However, the cell viability of *ApSK$_3$*-OE EC was significantly higher than that of the control group, while that in the *ApSK$_3$*-RNAi EC was noticeably lower than the control group after cryopreservation (Fig. 3a). Evan's blue detection showed that the cell relative death ratio of the control EC group was 50.43%, while the mortality of *ApSK$_3$*-OE EC was significantly reduced to 40.57%, and that *ApSK$_3$*-RNAi cells was significantly increased to 83.79% after cryopreservation treatment (Fig. 3b). The content of malondialdehyde (MDA), a product of membrane lipid peroxidation, increased continuously in EC during cryopreservation. The MDA content of *ApSK$_3$*-RNAi cells was significantly higher than that of control cells at osmo-protection and quick thawing stages, and the MDA content of *ApSK$_3$*-OE EC was significantly lower than the control group after cryopreservation (Fig. 3c). These results suggest that ApSK$_3$ can alleviate damage due to membrane lipid peroxidation during cryopreservation. Furthermore, ROS metabolism also changed significantly between the three EC genotypes (Fig. 3). H_2O_2 and OH· levels in *ApSK$_3$*-RNAi cells were significantly higher than in the other two EC genotypes. However, H_2O_2 and OH· had no significant difference between the control and *ApSK$_3$*-OE groups during cryopreservation treatments (Figs. 3d and 3e). Additionally, antioxidant enzyme SOD activity was significantly decreased in *ApSK$_3$*-RNAi cells (Fig. 3g), and non-enzymatic antioxidants AsA and GSH contents increased significantly in the *ApSK$_3$*-OE group during the whole cryopreservation process (Figs. 3h and 3i).

To evaluate the effect of ApSK$_3$ on the response of antioxidant system-related genes during cryopreservation, *catalase* (*CAT*), *Cu/ZnSOD*, *FeSOD*, *POD*, *glutathione peroxidase* (*GPX*), and *ascorbate peroxidase* (*APX*) were selected for gene quantitative expression analysis. *Cu/ZnSOD*, *FeSOD*, *POD*, and *GPX* of *ApSK$_3$*-OE EC were significantly up-regulated than in other groups at dehydration and quick thawing stages, and the expression of these genes did not differ significantly between the control and *ApSK$_3$*-RNAi groups (Fig. 4). *CAT* and *APX* were up-regulated in the *ApSK$_3$*-OE sample only during the quick thawing stage (Figs. 4a and 4f), and *APX* and *GPX* of *ApSK$_3$*-RNAi cells were significantly down-regulated compared to other

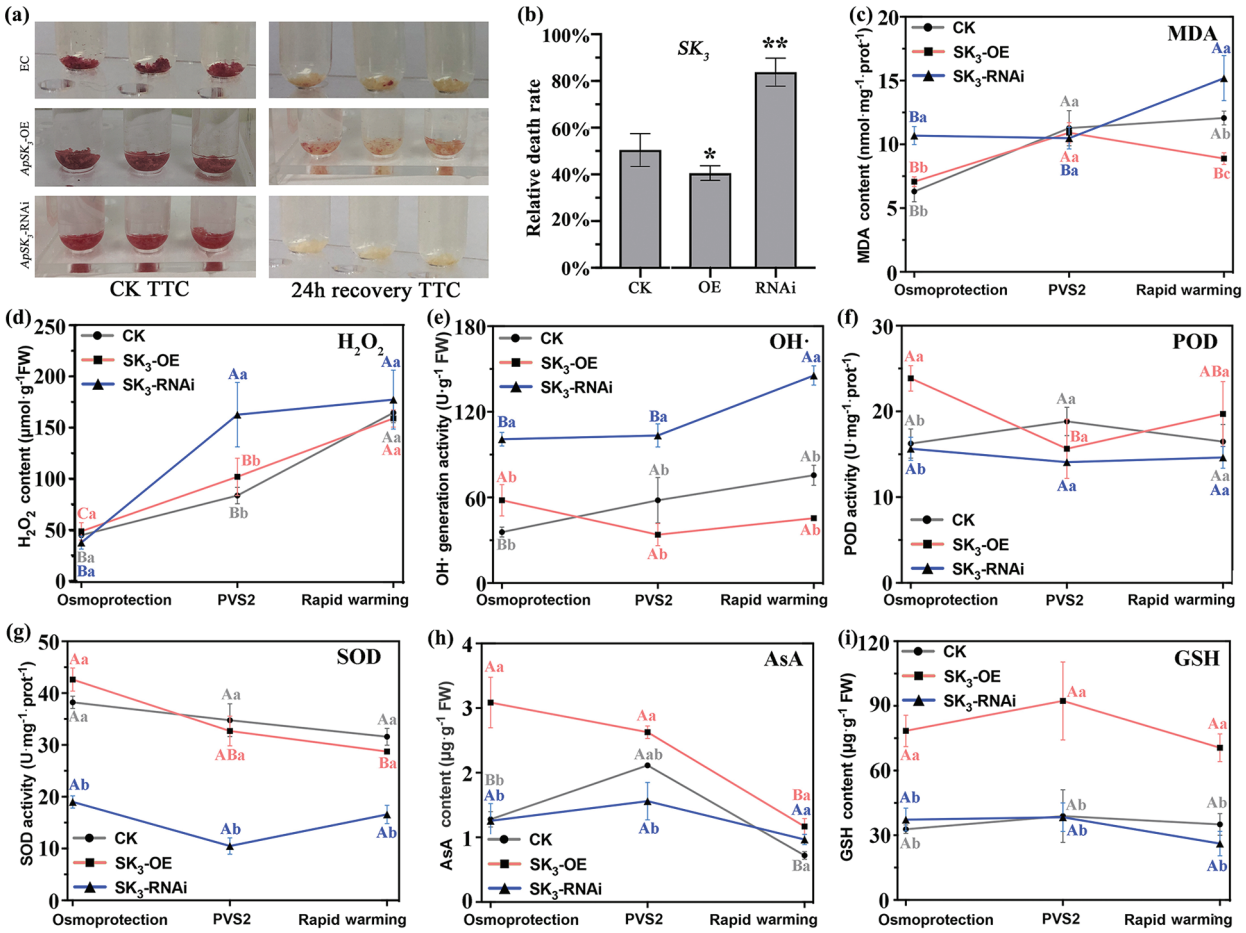

FIGURE 3. Changes of cell viability and stress physiological indexes of different genotypic *Agapanthus praecox* embryogenic callus during cryopreservation. Capital letters indicate that the same genotype embryogenic calluses have significant differences at different steps of cryopreservation; lower-case letters represent that the different genotype embryogenic calluses have significant differences at the same steps of cryopreservation. $^{*}P < 0.05$, $^{**}P < 0.01$.

groups in the later stages of cryopreservation (Figs. 4e and 4f). These results indicate that antioxidant systems related genes in *ApSK*$_3$-OE EC responded positively to cryopreservation complex stresses, and inhibition of *ApSK*$_3$ expression affects the GPX cycle and AsA–GSH cycle-related genes.

Correlation analysis of stress physiological indexes between the three genotypic cells was performed to reveal the direct or indirect protective function of *ApSK*$_3$ in cryopreservation (Table 1). The results show that, in the control group, the level of OH· correlated negatively with SOD, *Cu/ZnSOD*, and *POD*. SOD activity had a significant positive correlation to *Cu/ZnSOD* and *POD* expression level, and *GPX* was negatively correlated with AsA. However, in the *ApSK*$_3$-OE group, MDA contents presented a significant negative correlation with OH· and POD and a significant positive correlation with GSH. Strikingly, in the *ApSK*$_3$-RNAi group, MDA contents had a significant positive correlation with OH· generation, H_2O_2 was negatively correlated with *APX*, and SOD was positively correlated with *GPX* (Table 1). Therefore, the correlation of membrane lipid peroxidation level and OH· generation activity during cryopreservation had significant differences among the three different *ApSK*$_3$ genotypic cells. The gene expression levels of *SOD*, *GPX*, and *APX* had a positive response to the above-mentioned changes.

Discussion

DHNs are accumulated during the late stages of seed development and are involved in various environmental stresses (Dure and Galau, 1981; Hernández-Sánchez *et al.*, 2014). DHNs response to stress protection has been well studied in several plant species, such as *Oryza sativa* (Lee *et al.*, 2005), *Citrus unshiu* (Hara *et al.*, 2005), *Hordeum vulgare* (Kosová *et al.*, 2008), *Populus trichocarpa* (Liu *et al.*, 2012), *Vitis vinifera* (Yang *et al.*, 2012), *Solanum habrochaites* (Liu *et al.*, 2015), *Hevea brasiliensis* (Cao *et al.*, 2017), and *Arabidopsis thaliana* (Nguyen *et al.*, 2020). Various investigations have indicated that the SKn type DHNs impart plant stress tolerance by improving ROS detoxification and reducing lipid peroxidation (Cao *et al.*, 2017; Riyazuddin *et al.*, 2021). Overexpression of two SKn type DHNs from *Hevea brasiliensis* increased proline accumulation, reduced H_2O_2 content, and alleviated electrolyte leakage in *Arabidopsis thaliana* under osmotic and drought stress (Cao *et al.*, 2017). In *Solanum habrochaites*, the SK$_3$-type DHN (ShDHN) is regulated by drought, salt, and cold stress, and its ectopic expression reduces H_2O_2 accumulation, alters the expression of several antioxidant genes including *POD*, *SOD*, and *GST*, and alleviated membrane damage in tomato (Liu *et al.*, 2015). In

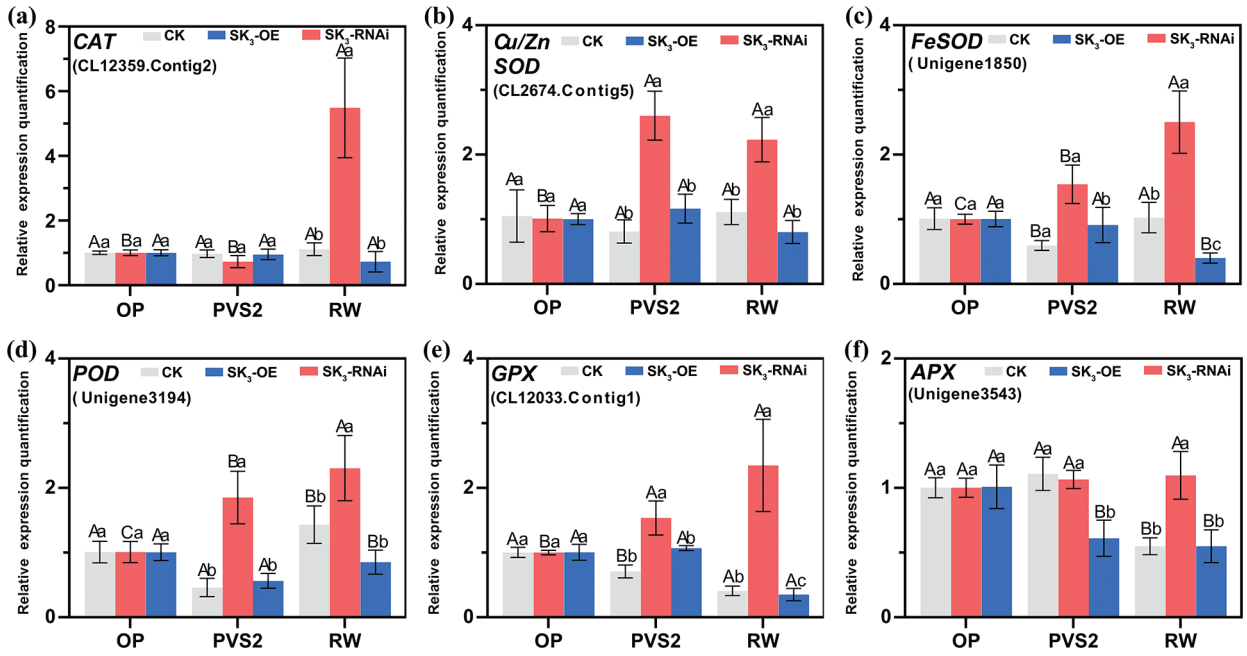

FIGURE 4. Real-time PCR quantitative analysis of antioxidant system-related genes of *ApSK$_3$* transgenic embryogenic callus (EC). *CAT*: catalase; *SOD*: superoxide dismutase; *POD*: peroxidase; *GPX*: glutathione peroxidase; *APX*: ascorbate peroxidase. *OP*: osmo-protection; *PVS2*: immersed in PVS2 (dehydration); *RW*: rapid warming (quick thawing). Capital letters indicate that ECs of the same genotype have significant differences at different steps of cryopreservation; lower-case letters represent that ECs of different genotypes have significant differences at the same steps of cryopreservation.

Agapanthus praecox, ApSK$_3$ was differentially expressed at both transcription and protein levels during the cryopreservation procedure and considered associated with the complex stress response. Ectopic expression of *ApSK$_3$* in *Arabidopsis thaliana* could alleviate oxidative damage and promote post-cryopreservation survival. The *ApSK$_3$* transgenic plants showed better growth status than wild-type *Arabidopsis thaliana* under osmotic and salt stress, with less ROS accumulation, higher antioxidant enzyme activity, greater accumulation of proline, and lower degrees of membrane lipid peroxidation (Yang *et al.*, 2019). Additionally, *in vitro* addition of ApSK$_3$ protein to PVS2 (a cryoprotectant) doubled the survival rate of *Arabidopsis thaliana* seedlings and significantly decreased the content of MDA and H_2O_2 (Zhang *et al.*, 2021). However, *in vitro* application of dehydrin, whether these proteins can cross the cell membrane into the plant cells and play a physiological protective role is still unclear. In this study, the cell viability of *Agapanthus praecox* EC, after cryopreservation, showed a completely opposite trend between overexpression and RNAi transgenic cell lines. Overexpression of *ApSK$_3$* enhanced the cell viability, non-enzymatic antioxidant (AsA and GSH) content, the expression level of antioxidant system-related genes, and affected the ROS metabolism during cryopreservation (Figs. 3 and 4). Down-regulated *ApSK$_3$* reduced the cell viability, antioxidant enzyme activities, and the expression level of antioxidant system-related genes, and significantly increased OH· generation activity during cryopreservation. Therefore, *in vivo* protective function of ApSK$_3$ can significantly improve the cell viability and antioxidant system, and alleviate oxidative stress damage during cryopreservation.

The molecular shielding model is an important hypothesis explaining the mechanism of the protective functions of biomacromolecules such as enzymes and proteins (Chakrabortee *et al.*, 2012; Hara *et al.*, 2016; Hughes *et al.*, 2013). *ApSK$_3$* dehydrin genetic transformation experiment in cryopreservation complex stresses supports the above model hypothesis (Yang *et al.*, 2019). Hara *et al.* (2003) investigated the effects of DHNs on lipid peroxidation and found that CuCOR19 of *Citrus unshiu* could prevent the oxidation of liposomes most likely by scavenging ROS. Several research groups have also demonstrated that, in addition to membranes, diverse DHNs are able to bind to many small ions and ligands (Kovacs *et al.*, 2008) and buffer the increase in ion concentration during dehydration stress. In this study, H_2O_2 and OH· levels had no significant difference between control and *ApSK$_3$*-OE groups during cryopreservation. However, OH· levels in *ApSK$_3$*-RNAi cells were significantly higher than in control and *ApSK$_3$*-OE ECs. Additionally, there was a significant positive correlation between MDA and OH· generation activity in the *ApSK$_3$*-RNAi group, while a significant negative correlation was found in the *ApSK$_3$*-OE group. ApSK$_3$ has a stronger Cu^{2+} and Fe^{3+} binding function and effectively inhibits the Fenton Reaction (H_2O_2 to OH·) (Yang *et al.*, 2019). Zhang *et al.* (2015) reported that OH· is a highly reactive and toxic chemical species in cells, and H_2O_2 is the main ROS component mediating oxidative damage and affecting cell viability during plant cryopreservation. Accordingly, these clues indicate that ApSK$_3$ can affect ROS metabolism through chelating metal ions and decreasing the damage of H_2O_2 and OH· to plant cells during cryopreservation.

We compared the effects of *in vitro* addition (Zhang *et al.*, 2021) and *in vivo* genetic transformation of ApSK$_3$ on cell viability after cryopreservation. Both methods could significantly improve cell viability and promote

TABLE 1

The correlation analysis of physiological indexes of stress and related genes of different genotypes of $ApSK_3$ during cryopreservation

CK	**MDA**	**H_2O_2**	**OH·**	**POD**	**SOD**	**AsA**	**GSH**	***CAT***	***CuZnSOD***	***FeSOD***	***POD***	***GPX***	***APX***
MDA	1	0.827	0.947	0.457	−0.931	−0.013	0.606	0.447	−0.952	−0.353	−0.921	0.054	−0.453
H_2O_2		1	0.963	−0.122	−0.975	−0.573	0.949	0.873	−0.960	0.234	−0.981	0.606	−0.876
OH·			1	0.149	**−0.999***	−0.333	0.829	0.710	**−1.000****	−0.035	**−0.997***	0.370	−0.715
POD				1	−0.100	0.883	−0.430	−0.591	−0.162	−0.993	−0.073	−0.864	0.586
SOD					1	0.379	−0.855	−0.744	**0.998***	−0.014	**1.000***	−0.416	0.748
AsA						1	−0.803	−0.900	0.320	−0.931	0.403	**−0.999***	0.897
GSH							1	0.982	−0.821	0.530	−0.869	0.826	−0.984
CAT								1	−0.700	0.679	−0.761	0.917	**−1.000****
CuZnSOD									1	0.049	0.996	−0.358	0.705
FeSOD										1	−0.041	0.915	−0.674
POD											1	−0.439	0.765
GPX												1	−0.914
APX													1
$ApSK_3$-OE	MDA	H_2O_2	OH·	POD	SOD	AsA	GSH	*CAT*	*CuZnSOD*	*FeSOD*	*POD*	*GPX*	*APX*
MDA	1	0.454	**−0.998***	**−0.999***	−0.670	−0.197	**1.000****	−0.085	0.945	0.324	0.363	0.614	0.630
H_2O_2		1	−0.508	−0.488	−0.966	−0.963	0.444	0.850	0.720	0.990	0.995	0.982	0.978
OH·			1	**1.000****	0.715	0.257	**−0.997***	0.022	−0.964	−0.382	−0.420	−0.662	−0.678
POD				1	−0.698	0.234	**−0.999***	0.046	−0.957	−0.360	−0.398	−0.644	−0.660
SOD					1	0.860	−0.661	−0.683	−0.875	−0.920	−0.935	**−0.997***	**−0.999***
AsA						1	−0.186	−0.960	−0.506	−0.991	−0.985	−0.894	−0.885
GSH							1	−0.096	0.942	0.314	0.353	0.606	0.622
CAT								1	0.245	0.915	0.898	0.734	0.720
CuZnSOD									1	0.615	0.647	0.838	0.849
FeSOD										1	**0.999***	0.946	0.939
POD											1	0.958	0.952
GPX												1	**1.000***
APX													1
$ApSK_3$-RNAi	MDA	H_2O_2	OH·	POD	SOD	AsA	GSH	*CAT*	*CuZnSOD*	*FeSOD*	*POD*	*GPX*	*APX*
MDA	1	0.623	**1.000****	−0.220	0.190	−0.830	−0.991	−0.992	0.868	−0.996	−0.991	0.123	−0.645
H_2O_2		1	0.622	−0.900	−0.649	−0.82	−0.512	−0.717	−0.153	−0.690	−0.512	−0.700	**−1.000***
OH·			1	−0.218	0.192	−0.831	−0.991	−0.992	−0.869	−0.996	−0.991	0.124	−0.644
POD				1	0.916	−0.362	0.086	0.341	−0.293	0.305	0.086	0.941	0.887
SOD					1	−0.705	−0.321	−0.065	−0.652	−0.103	−0.321	**0.998***	0.628
AsA						1	0.898	0.753	**0.997***	0.778	0.898	−0.655	0.109
GSH							1	0.966	0.927	0.975	**1.000****	−0.256	0.535
CAT								1	0.799	**0.999***	0.966	0.003	0.736
CuZnSOD									1	0.821	0.927	−0.599	0.180
FeSOD										1	0.975	−0.034	0.710
POD											1	−0.255	0.536
GPX												1	0.680
APX													1

Note: Bold values indicate a significant correlation between the two indices (* $p < 0.05$, ** $p < 0.01$).

post-cryopreservation survival, and the protective mechanisms of dehydrin were similar *in vitro* and *in vivo*. The main difference between the above two methods, including *in vitro* added $ApSK_3$ to PVS, has a better effect on reducing intracellular H_2O_2 content, and *$ApSK_3$* transgenic cells have more beneficial in reducing OH· damage and protecting the activity of antioxidant enzymes during cryopreservation. These results indicate that $ApSK_3$ dehydrin can effectively

enhance the stress resistance of plants and has great potential for both *in vitro* and *in vivo* applications in plant cryopreservation.

Materials and Methods

Plant materials

EC of *Agapanthus praecox* was induced from pedicel tissue, according to Zhang *et al.* (2015). EC was continuously sub-cultured in the dark on Murashige and Skoog (MS) medium supplemented with 1.5 mg·L^{-1} picloram (Sangon Biotech, Shanghai, China) at 25°C.

Plasmid construction and genetic transformation

The gene sequence of SK$_3$ was obtained from Yang *et al.* (2019). The gene open reading frame (ORF) and RNAi sequence of *ApSK$_3$* were amplified by gene-specific primers. The digestion sites of the CDS sequence are *SpeI* and *BamHI*, and the digestion sites of the *ApSK$_3$* RNAi sequence are *SacI*/*BamHI* and *KpnI*/*SpeI* (Table 2). RNAi and ORF sequence of *ApSK$_3$* were ligated to pTCK303 and pHB vectors, respectively, by enzyme digestion (Chen *et al.*, 2021; Yuan *et al.*, 2014). The recombinant plasmids (pHB-YFP-ApSK$_3$ and pTCK303-ApSK$_3$) were transferred into the EC by the GV3101-mediated method. The transgenic materials were screened for hygromycin resistance (Sangon Biotech, Shanghai, China), and stable growth calluses were obtained for further study. Quantitative real-time PCR and western blot analysis were used to verify the mRNA and protein level of ApSK$_3$ in all transgenic lines. The YFP signals of overexpression transgenic EC were observed by laser-scanning confocal microscopy (Leica TCS SP5II, Wetzlar, Germany), according to Yang *et al.* (2019). The GUS staining of RNAi transgenic EC was performed by Jefferson *et al.* (1987).

Cryopreservation

Pre-culture: the EC of *Agapanthus praecox* was placed on the pre-culture solid medium (0.5 M sucrose MS medium), 4°C, in the dark for 2 days. For loading: 0.2 g of EC was placed onto the cryopreservation tube, and 2 mL loading solution was added and treated at 25°C for 1 h. For dehydration: the loading liquid was completely removed, and 2 mL of cryoprotectant (PVS2) was added and treated at 0°C on ice for 40 min. For rapid freezing: the cryopreservation tube was placed in liquid nitrogen for 1 h; for quick thawing, it was placed in a 40°C water bath for 90 s. This was washed using a washing solution to remove PVS2 solution for 30 min, and fresh washing solution was replaced every 10 min. For the recovery of culture: ECs were transferred to a solid subculture medium, and the residual washing solution was sucked and treated at 25°C in the dark for 1 d. The preparation of media and solutions were according to Zhang *et al.* (2015).

Western blot assay

Western blot analysis was performed as previously described (Yang *et al.*, 2019). To resolve the proteins, sodium dodecyl

TABLE 2

The primers used for ApSK$_3$ amplified sequence for overexpression and RNAi vector construction and qRT-PCR

Primers	Sequence (5'–3')	Tm (°C)
SK$_3$-OE-S	AAGGATCCATGGCAGAGGAGAATGTGGA	64.9
SK$_3$-OE-A	AACTAGTCTAATGAGCCTTCTCGGTCTC	63.5
SK$_3$-RNAi-S	GGGGTACCACTAGTAGGGTTGTTTGGTTTCGTGG	66.9
SK$_3$-RNAi-A	CGGGATCCGAGCTCTTTCTTCGCCTCCTCAAC	68.6
Ap-Actin-s	CAGTGTCTGGATTGGAGG	50.6
Ap-Actin-a	TAGAAGCACTTCCTGTG	50.3
RT-SK$_3$-s	CTTCTTCTCGCCGTCTTC	55.1
RT-SK$_3$-a	AAGAGCCAAGAGGAGGTT	55.2
CAT-s	GGCACTTGCACCTCTTGC	57.2
CAT-a	ACCACTTTCACCACCACC	54.9
Cu-ZnSOD-s	GCAGTGAGGGAGTGAAGG	57.2
Cu-ZnSOD-a	TGCAGCCATTTGTGGTAT	50.3
FeSOD-s	GCTCCTGCATTCCCTGTG	57.2
FeSOD-a	AACATTGTGGCCGACGAA	52.6
POD-s	ACAACCCTTGTCTATTCACG	53.4
POD-a	TTCACCAACCGCCTCTAC	54.9
GPX-s	CATGGGAAAGCCAGGATC	54.9
GPX-a	CGATTTCACCGTCAAGGA	52.6
APX-s	ACAAGCGGGCGGAAGACA	57.2
APX-a	TGGGCAGGTGCCACAAAG	57.2

sulfate-polyacrylamide gel (12% for separation and 8% stacking gel) was prepared. Twenty microliters of protein samples were added to the well and separated at 90 V for 30 min and then at 80 V for 90 min. After electrophoresis, the gel was removed, rinsed with deionized water, placed in the film transfer fluid, and balanced for 15 min. For membrane transfer, a 0.22 μM PVDF membrane (Amersham Pharmacia, Shanghai, China) was used to transfer the protein at 30 V and 4°C for 3 h. The membrane was blocked with 5% nonfat milk for 3 h, and GFP primary antibody (Sangon Biotech, Shanghai, China) was added to the diluent containing the membrane for 3 h. The membrane was washed with TBST buffer for 30 min. Then, the secondary antibody diluent (Sangon Biotech, Shanghai, China) was added.

Assay for cell viability and cell death

The survival of cryopreserved cells was assessed by the TTC method. EC tissue (100 mg) was immersed into 2 mL of TTC (Sangon Biotech, Shanghai, China) buffer (0.8% TTC in 0.05 M PBS) and incubated in the dark at 25°C for 20 h. EC cells were rinsed thrice with 2 mL sterile water. The staining state of the EC was captured using a Nikon camera.

Evan's blue assay was performed according to Chen *et al.* (2021). EC (100 mg) was suspended in 0.05% Evan's blue solution and incubated for 15 min at 25°C. Cells were collected by centrifugation at 16,000 g for 5 min and washed with distilled water until no more dye was eluted. The trapped dye was then released by adding 1.0 mL of 1% SDS at 80°C for 1 h. The supernatant was detected at an absorbance of 600 nm by a spectrophotometer (Thermo Biomate160).

Detection of physiological indices

The contents of MDA, H_2O_2, OH·, and GSH and the activity of POD, SOD, AsA and GSH were detected using their respective test kits (Nanjing Jiancheng Bioengineering Institute, Nanjing, China) (Yang *et al.*, 2019).

Total RNA extraction and quantitative real-time PCR

The total RNA was extracted using the TaKaRa plant RNA extraction kit (TaKaRa, Shanghai, China). RNA was then reverse transcribed to cDNA using the RT reagent kit (TaKaRa, Shanghai, China). qRT-PCR was performed in an ABI 7900 HT RT-PCR detection system (Thermo Fisher Scientific, Boston, USA). Amplification was carried out using Brilliant SYBR Green QPCR Master Mix (Takara, Shanghai, China) according to the manufacturer's instructions. The relative quantification of transcript abundance was calculated using the $2^{-\Delta\Delta CT}$ method. The ID of genes related to antioxidant system are as follows: *CAT* (CL12359.Contig2), *Cu/Zn SOD* (CL2674.Contig5), *FeSOD* (Unigene1850), *POD* (Unigene3194), *GPX* (CL12033.Contig1), and *APX* (Unigene3543). The primer sequences used for qRT-PCR are listed in Table 2. *ApActin* was used as the endogenous control.

Statistical analysis

All experiments had more than three different biological replicates, and experimental data were expressed as the mean ± SD. The correlation analyses and statistical comparisons were determined by SPSS (Version 20.0, USA). Differences in parameters were analyzed, and their level of significance was calculated by using one-way ANOVA. Data were visualized using GraphPad Prism (Version 9.0, USA).

Availability of Data and Materials: All data generated or analyzed during this study are included in this published article.

Author Contribution: Study conception and design: Di Zhang; data collection: Tingting Huang and Shan Deng; analysis and interpretation of results: Tingting Huang and Jiangyuan Sheng; draft manuscript: Di Zhang and Tingting Huang. All authors reviewed the results and approved the final version of the manuscript.

Ethics Approval: Not applicable.

Funding Statement: This work was supported by the National Natural Science Foundation of China [Grant Nos. 31870686, 31971705, and 31670693] and the Natural Science Foundation of Shanghai [Grant No. 21ZR1434200].

Conflicts of Interest: The authors declare that they have no conflicts of interest to report regarding the present study.

References

Abdul AM, Sabeem M, Mullath SK, Brini F, Masmoudi K (2021). Plant group II LEA proteins: Intrinsically disordered structure for multiple functions in response to environmental stresses. *Biomolecules* **9**: 1662.

Avelange-Macherel MH, Payet N, Lalanne D, Neveu M, Tolleter D, Burstin J, Macherel D (2015). Variability within a pea core collection of LEAM and HSP22, two mitochondrial seed proteins involved in stress tolerance. *Plant Cell and Environment* **38**: 1299–1311.

Bao F, Du D, An Y, Yang W, Wang J, Cheng T, Zhang Q (2017). Overexpression of *Prunus mume* dehydrin genes in tobacco enhances tolerance to cold and drought. *Frontiers in Plant Science* **8**: 1299–1311.

Cao Y, Xiang X, Geng M, You Q, Huang X (2017). Effect of *HbDHN1* and *HbDHN2* genes on abiotic stress responses in *Arabidopsis*. *Frontiers in Plant Science* **8**: 470.

Chakrabortee S, Tripathi R, Watson M, Schierle GS, Kurniawan DP et al. (2012). Intrinsically disordered proteins as molecular shields. *Molecular BioSystems* **8**: 210–219.

Chen G, Zhang D, Pan J, Yue J, Shen X (2021). Cathepsin B-like cysteine protease *ApCathB* negatively regulates cryo-injury tolerance in transgenic *Arabidopsis* and *Agapanthus praecox*. *Plant Science* **308**: 110928.

Close TJ (1997). Dehydrins: A commonality in the response of plants to dehydration and low temperature. *Plant Physiology* **100**: 291–296.

Dure L, Galau GA (1981). Developmental biochemistry of cotton seed embryogenesis and germination XIII. Regulation of biosynthesis of principal storage proteins. *Plant Physiology* **68**: 187–194.

Elliott GD, Wang S, Fuller BJ (2017). Cryoprotectants: A review of the actions and applications of cryoprotective solutes that modulate cell recovery from ultra-low temperatures. *Cryobiology* **76**: 74–91.

Fayter AER, Hasan M, Congdon TR, Kontopoulou I, Gibson MI (2020). Ice recrystallisation inhibiting polymers prevent irreversible protein aggregation during solvent-free cryopreservation as

additives and as covalent polymer-protein conjugates. *European Polymer Journal* **140**: 110036.

Halder T, Agarwal T, Ray S (2016). Isolation, cloning, and characterization of a novel *Sorghum* dehydrin (*SbDhn2*) protein. *Protoplasma* **253**: 1475–1488.

Hara M, Terashima S, Fukaya T, Kuboi T (2003). Enhancement of cold tolerance and inhibition of lipid peroxidation by citrus dehydrin in transgenic tobacco. *Planta* **217**: 290–298.

Hara M, Fujinaga M, Kuboi T (2005). Metal binding by citrus dehydrin with histidine-rich domains. *Journal of Experimental Botany* **56**: 2695–2703.

Hara M, Monna S, Murata T, Nakano T, Amano S, Nachbar M, Wätzig H (2016). The *Arabidopsis* KS-type dehydrin recovers lactate dehydrogenase activity inhibited by copper with the contribution of his residues. *Plant Science* **245**: 135–142.

Hernández-Sánchez IE, Martynowicz DM, Rodríguez-Hernández AA, Pérez-Morales MB, Graether SP, Jimenez-Bremont JF (2014). A dehydrin-dehydrin interaction: The case of SK$_3$ from *Opuntia streptacantha*. *Frontiers in Plant Science* **5**: 520.

Hoekstra FA, Golovina EA, Buitink J (2001). Mechanisms of plant desiccation tolerance. *Trends in Plant Science* **6**: 431–438.

Hughes SL, Schart V, Malcolmson J, Hogarth KA, Martynowicz DM, Tralman-Baker E, Patel SN, Graether SP (2013). The importance of size and disorder in the cryoprotective effects of dehydrins. *Plant Physiology* **163**: 1376–1386.

Jefferson RA, Kavanagh TA, Bevan MW (1987). GUS fusions: β-glucuronidase as a sensitive and versatile gene fusion marker in higher plants. *The EMBO Journal* **6**: 3901–3907.

Kosová K, Holková L, Prásil IT, Prásilová P, Bradácová M, Vítámvás P, Capková V (2008). Expression of dehydrin 5 during the development of frost tolerance in barley (*Hordeum vulgare*). *Journal of Plant Physiology* **165**: 1142–1151.

Kovacs D, Kalmar E, Torok Z, Tompa P (2008). Chaperone activity of ERD10 and ERD14, two disordered stress-related plant proteins. *Plant Physiology* **147**: 381–390.

Lee SC, Lee MY, Kim SJ, Jun SH, An G, Kim SR (2005). Characterization of an abiotic stress-inducible dehydrin gene, *OsDhn1*, in rice (*Oryza sativa* L.). *Molecules and Cells* **19**: 212–218.

Liu CC, Li CM, Liu BG, Ge SJ, Dong X (2012). Genome-wide identification and characterization of a dehydrin gene family in poplar (*Populus trichocarpa*). *Plant Molecular Biology Reporter* **30**: 848–859.

Liu H, Yu C, Li H, Ouyang B, Wang T, Zhang J, Wang X, Ye Z (2015). Overexpression of *ShDHN*, a dehydrin gene from *Solanum habrochaites* enhances tolerance to multiple abiotic stresses in tomato. *Plant Science* **231**: 198–211.

Liu Y, Wang L, Xing X, Sun L, Pan J, Kong X, Zhang M, Li D (2013). ZmLEA$_3$, a multifunctional group 3 LEA protein from maize (*Zea mays* L.), is involved in biotic and abiotic stresses. *Plant and Cell Physiology* **54**: 944–959.

Livernois AM, Hnatchuk DJ, Findlater EE, Graether SP (2009). Obtaining highly purified intrinsically disordered protein by boiling lysis and single step ion exchange. *Analytical Biochemistry* **392**: 70–76.

Meryman HT (2007). Cryopreservation of living cells: Principles and practice. *Transfusion* **47**: 935–945.

Nguyen PN, Tossounian MA, Kovacs DS, Thu TT, Stijlemans B et al. (2020). Dehydrin ERD14 activates glutathione transferase Phi9 in *Arabidopsis thaliana* under osmotic stress. *Biochimica et Biophysica Acta (BBA)-General Subjects* **3**: 129506.

Rakhra G, Kaur T, Vyas D, Sharma AD, Singh J, Ram G (2017). Molecular cloning, characterization, heterologous expression and *in-silico* analysis of disordered boiling soluble stress-responsive wBsSRP protein from drought tolerant wheat cv. PBW 175. *Plant Physiology and Biochemical Journal* **112**: 29–44.

Reed BM (2001). Implementing cryogenic storage of clonally propagated plants. *Cryo-Letters* **22**: 97–104.

Ren L, Zhang D, Jiang X, Gai Y, Wang W, Reed BM, Shen X (2013). Peroxidation due to cryoprotectant step is a vital factor for cell survival in *Arabidopsis* cryopreservation. *Plant Science* **212**: 37–47.

Ren L, Zhang D, Shen X, Reed BM (2014). Antioxidants and anti-stress compounds improve the survival of cryopreserved *Arabidopsis* seedlings. *Acta Horticulturae* **1039**: 57–62.

Ren L, Zhang D, Chen G, Reed BM, Shen X, Chen H (2015). Transcriptomic profiling revealed the regulatory mechanism of *Arabidopsis* seedlings response to oxidative stress from cryopreservation. *Plant Cell Reports* **34**: 2161–2178.

Ren L, Wang MR, Wang QC (2021). ROS-induced oxidative stress in plant cryopreservation: Occurrence and alleviation. *Planta* **254**: 124.

Riyazuddin R, Nisha N, Singh K, Verma R, Gupta R (2021). Involvement of dehydrin proteins in mitigating the negative effects of drought stress in plants. *Plant Cell Reports* **41**: 519–533. DOI 10.1007/s00299-021-02720-6.

Saibi W, Feki K, Mahmoud RB, Brini F (2015). Durum wheat dehydrin (DHN-5) confers salinity tolerance to transgenic *Arabidopsis* plants through the regulation of proline metabolism and ROS scavenging system. *Planta* **242**: 1187–1194.

Sakai A, Dai H, Niino T (2008). Development of pvs-based vitrification and encapsulation-vitrification protocols. In: *Plant Cryopreservation: A Practical Guide*, pp. 33–57. New York: Springer.

Saucedo AL, Hernández-Domínguez EE, de Luna-Valdez LA, Guevara-García AA, Escobedo-Moratilla A et al. (2017). Insights on structure and function of a late embryogenesis abundant protein from *Amaranthus cruentus*: An intrinsically disordered protein involved in protection against desiccation, oxidant conditions, and osmotic stress. *Frontiers in Plant Science* **8**: 497.

Smolikova G, Leonova T, Vashurina N, Frolov A, Medvedev S (2020). Desiccation tolerance as the basis of long-term seed viability. *International Journal of Molecular Medicine* **22**: 101.

Yang Y, He M, Zhu Z, Li S, Xu Y et al. (2012). Identification of the dehydrin gene family from grapevine species and analysis of their responsiveness to various forms of abiotic and biotic stress. *BMC Plant Biology* **12**: 140.

Yang Z, Sheng J, Lv K, Ren L, Zhang D (2019). Y$_2$SK$_2$ and SK$_3$ type dehydrins from *Agapanthus praecox* can improve plant stress tolerance and act as multifunctional protectants. *Plant Science* **284**: 143–160.

Yuan F, Chen M, Yang J, Leng B, Wang B (2014). A system for the transformation and regeneration of the recretohalophyte *Limonium bicolor*. *In Vitro Cellular and Developmental Biology* **50**: 610–617.

Zamecnik J, Faltus M, Bilavcik A (2021). Vitrification solutions for plant cryopreservation: Modification and properties. *Plants* **10**: 2623.

Zhang D, Ren L, Chen G, Zhang J, Reed BM, Shen X (2015). ROS-induced oxidative stress and apoptosis-like event directly affect the cell viability of cryopreserved embryogenic callus in *Agapanthus praecox*. *Plant Cell Reports* **34**: 1499–1513.

Zhang D, Yang T, Ren L (2021). Y$_2$SK$_2$ and SK$_3$ type dehydrins from *Agapanthus praecox* act as protectants to improve plant cell viability during cryopreservation. *Plant Cell, Tissue and Organ Culture* **144**: 271–279.